

The Evolution of Siphonophore Tentilla as Specialized Tools for Prey Capture

Alejandro Damian-Serrano^{1,‡}, Steven H.D. Haddock², Elizabeth D. Hetherington³, C. Anela Choy³, Casey W. Dunn¹

¹ Osborn Memorial Laboratories, Department of Ecology and Evolutionary Biology, 165 Prospect St., Yale University, New Haven, CT 06520, USA

² Monterey Bay Aquarium Research Institute, 7700 Sandholdt Rd., Moss Landing, CA 95039, USA

³ Scripps Institution of Oceanography, 9500 Gilman Dr., La Jolla, CA 92093, USA

‡ Corresponding author: Alejandro Damian-Serrano, email: alejandro.damianserrano@yale.edu

Abstract

Predators have evolved dedicated body parts to capture and subdue prey. As different lineages specialize on distinct prey taxa, their tools for prey capture diverge into a variety of adaptive forms. Studying this process requires a predator clade with structures used exclusively for prey capture that present significant morphological variation. Siphonophores, a clade of colonial cnidarians, satisfy these criteria particularly well, capturing prey with their tentilla (tentacle side branches). Earlier work has shown that extant siphonophore diets correlate with the different morphologies and sizes of their tentilla and nematocysts. We hypothesize that evolutionary specialization on different prey types has driven the phenotypic evolution of these characters. To test this hypothesis, we: (1) measured extensive morphological traits from fixed siphonophore specimens using microscopy and high speed video techniques, (2) built a phylogenetic tree of 45 species, and (3) characterized the evolutionary associations between siphonophore nematocyst characters and prey type data from the literature. Our results show that siphonophore tentilla structure has strong evolutionary associations with prey type and size specialization, and suggest that shifts between prey type specializations are linked to shifts in tentillum and nematocyst size and shape. In addition, we found that these morphological characters are useful for predicting siphonophore diets. Thus, the evolutionary history of tentilla shows that siphonophores are an example of ecological niche diversification via morphological innovation and evolution. This study contributes to understanding how morphological evolution has shaped the structure of present-day oceanic food-webs.

Keywords

Siphonophores, tentilla, nematocysts, predation, specialization, character evolution

Most animal predators have characteristic biological tools that they use to capture and subdue prey. Raptor birds have claws and beaks, snakes have fangs, wasps have stingers, and cnidarians have nematocyst-laden tentacles. The functional morphology of these structures tend to be finely attuned to their ability to successfully capture specific prey (Schmitz 2017). Long-term adaptive evolution in response to the defense mechanisms (e.g. avoidance, escape, protective barriers) of the prey leads to modifications that can tackle those defenses. The more specialized the diet of a predator is, the more specialized its tools need to be to meet the specific challenges posed by the prey. Understanding the relationships between predatory and morphological specializations is necessary to contextualize the phenotypic diversity of predators, and to quantify the importance of ecological diversification in generating this diversity.

Siphonophores (Cnidaria : Hydrozoa) are a clade of organisms bearing modular structures that are exclusively used for prey capture and present a significant morphological variation across species, which makes it ideal to study the relationships between functional traits and prey specialization. A siphonophore is a colony bearing many feeding polyps (Fig. 1), each with a single tentacle, which branches into several tentilla bearing the functional cnidocytes (specialized neural cells carrying nematocysts, the stinging capsules). Tentilla function exclusively for prey capture and present a broad diversity of morphologies and sizes (Mapstone 2014). Unlike most other cnidarians, siphonophores carry their tentacle nematocysts in extremely complex and organized batteries (Skaer 1988), built into their tentilla. While nematocyst batteries and clusters in

other cnidarians are simple static scaffolds for cnidocytes, siphonophore tentilla have their own reaction mechanism upon encounter with prey. Tentilla undergo an extremely fast conformational change that wraps around the prey, maximizing the surface area of contact for nematocysts to fire on it (Mackie et al. 1987). In addition, some species have elaborate fluorescent and bioluminescent lures on their tentilla to attract prey with aggressive mimicry (Purcell 1980; Haddock et al. 2005).

Many siphonophore species inhabit the deep pelagic ocean, which spans from ~200m to the oceanic seafloor (~3000-11000m). This habitat has fairly homogeneous abiotic conditions and stable temporal patterns in the abundance of zooplanktonic animals (Robison 2004). With a somewhat predictable prey availability, ecological theory would expect evolution to drive coexisting siphonophore lineages towards specialization, increasing their feeding efficiencies and reducing interspecific competition (Hardin 1960; Hutchinson 1961). If this prediction holds true, we expect the prey capture apparatus morphologies of siphonophores to diversify with the evolution of specialization on a variety of prey types.

The study of siphonophore tentilla and diets has been limited in the past due to the inaccessibility of their oceanic habitat and the difficulties associated with the collection of fragile siphonophores. Thus, the morphological diversity of tentilla has been only characterized for a few taxa, and their evolutionary history remains largely unexplored. Contemporary underwater sampling technology provides an unprecedented opportunity to explore the trophic ecology (Choy et al. 2017) and functional morphology (Costello et al. 2015) of siphonophores. In addition, well-supported phylogenies based on molecular data are now available for these organisms (Munro et al. 2018). These methodological advances allow for the examination of relationships between modern siphonophore form, function, and ecology, as well as reconstructing their evolutionary history.

The few studies have addressed the relationships between tentilla and diet suggest that siphonophores are a robust system for the study of predatory specialization via morphological diversification. (Purcell 1984) and (Purcell and Mills 1988) showed clear relationships between diet, tentillum, and nematocyst characters in co-occurring epipelagic siphonophores. These correlations, while found in a small subset of extant epipelagic siphonophore species, might be generalizable to all siphonophores. We hypothesize that these relationships may reflect correlated evolution between prey selection and tentillum (and nematocyst) traits. Furthermore, we hypothesize that with an extensive characterization of tentilla morphology, we can generate predictions about the diets of understudied siphonophore species. In addition, our study design allows us to address other interesting questions about the morphology and evolution of these unique structures. We aim to assess the evolutionary origins of giant tentilla, the phenotypic integration of tentilla, the evolution of the extreme shapes of siphonophore haploneme nematocysts (Thomason 1988), and the mechanical implications of tentilla morphologies on cnidoband discharge.

In this study, we characterize the morphological diversity of tentilla and their nematocysts across a broad variety of shallow and deep sea siphonophore species using modern imaging technologies, we expand the phylogenetic tree of siphonophores by combining a broad taxon sampling of ribosomal gene sequences with a transcriptome-based backbone tree, and we explore the evolutionary histories and correlations among diet, tentillum, and nematocyst characters.

Methods

Tentilla morphology – The morphological work was carried out on siphonophore specimens fixed in 4% formalin from the Yale Peabody Museum Invertebrate Zoology (YPM-IZ) collection (catalog numbers in Appendix 1). These specimens had been collected intact across many years of fieldwork expeditions, by the means of blue-water Diving (Haddock and Heine 2005), remotely operated vehicles (ROVs), and human-operated submersibles. Tentacles were dissected from non-larval gastrozooids, sequentially dehydrated into 100% ethanol, cleared in methyl salicylate, and mounted into slides with Canada Balsam or Permount mounting media. The slides were imaged as tiled z-stacks using differential interference contrast (DIC) on an automated stage at YPM-IZ (with the assistance of Daniel Drew and Eric Lazo-Wasem) and laser point confocal microscopy using a 488 nm Argon laser that excited autofluorescence in the tissues. Thirty characters (defined in Appendix 2) were measured using Fiji (Collins 2007; Schindelin et al. 2012). We did not measure the lengths of contractile structures (terminal filaments, pedicles, gastrozooids, and tentacles), since they are too variable to capture meaningful measurements. We measured at least one specimen for 96 different species (Appendix 3, Fig. @{figure3}). Of these, we selected 38 focal siphonophore species based on specimen availability and phylogenetic representation from each clade. Three to five tentacle specimens from each one

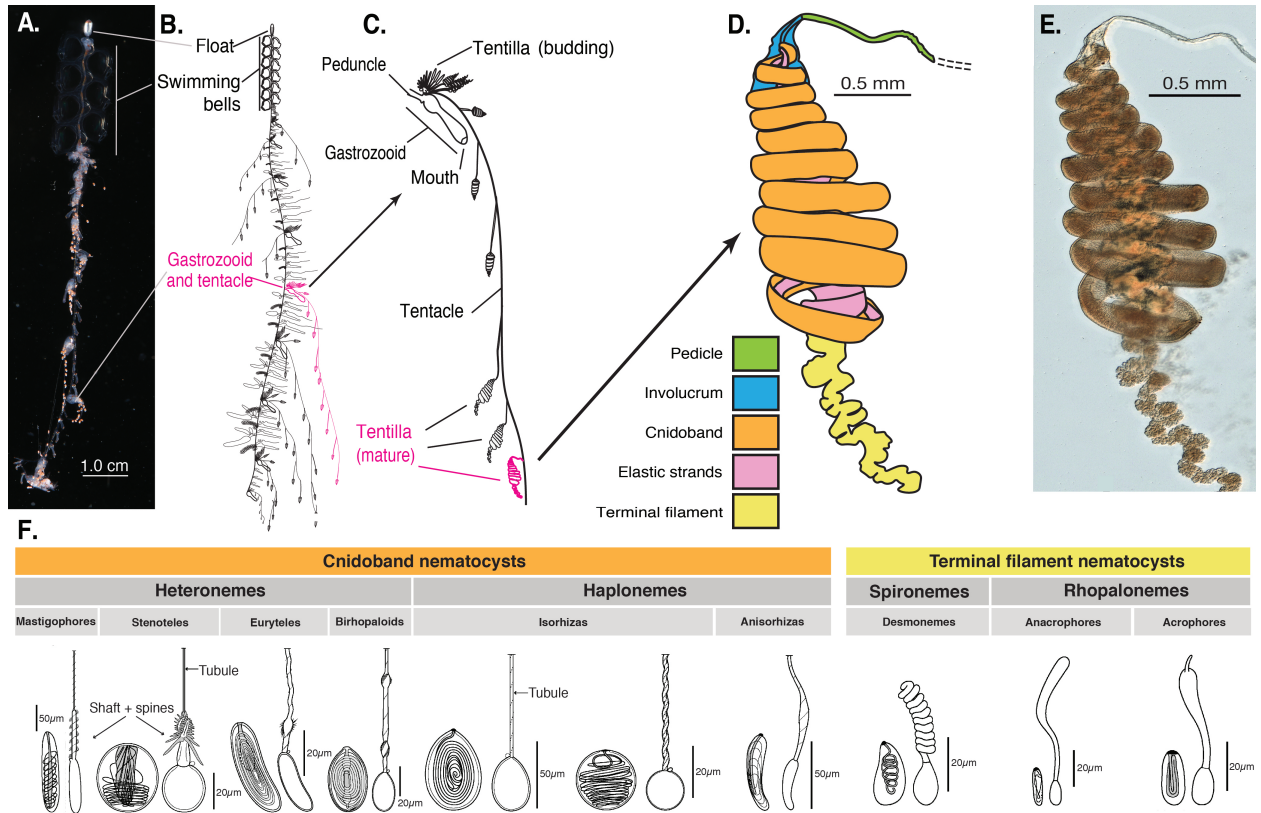


Figure 1: Siphonophore anatomy. A - *Nanomia* sp. siphonophore colony (photo by Catriona Munro). B,C - Illustration of a *Nanomia* colony, gastrozooid, and tentacle (by Freya Goetz). D - *Nanomia* sp. Tentillum illustration and main parts. E - Transmission micrograph of the tentillum illustrated in D. F - Nematocyst types (illustration reproduced with permission from Mapstone 2014), hypothesized homologies, and locations in the tentillum. Undischarged to the left, discharged to the right.

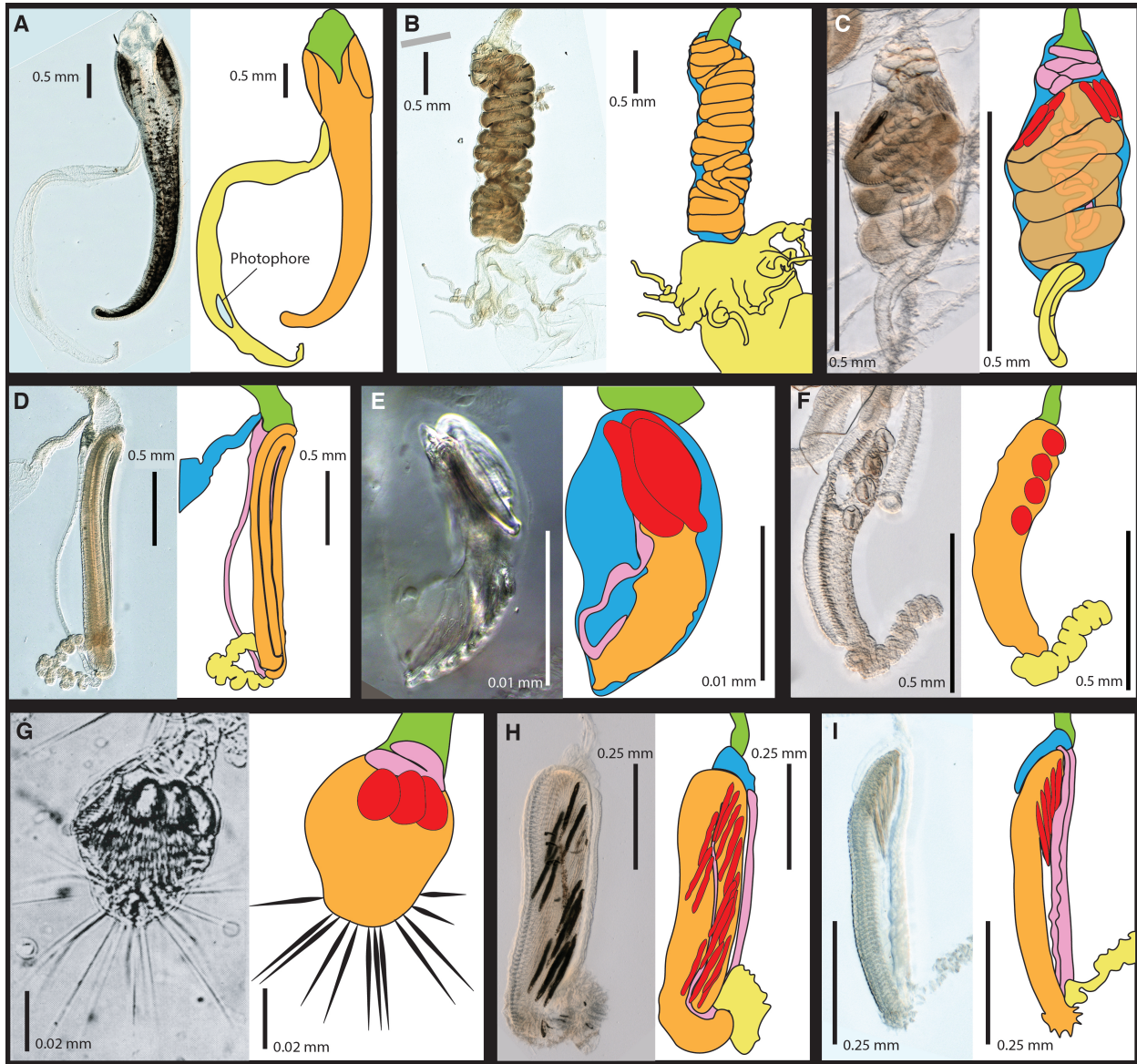


Figure 2: Tentillum diversity plate. The illustrations delineate the pedicle (green), involucrum (blue), cnidoband (orange), elastic strands (pink), terminal structures (yellow). Heteroneme nematocysts (stenoteles in C,E,F,G and mastigophores in H,I) are depicted in red for some species. A - *Erenna laciniata*, slide E11, 10x. B - *Lychnagalma utricularia*, slide D7, 10x. C - *Agalma elegans*, slide J6, 10x. D - *Resomia ornicephala*, slide X11, 10x. E - *Frillagalma vityazi*, slide H1, 20x. F - *Bargmannia amoena*, slide L8, 10x. G - *Cordagalma* sp., reproduced from Carré 1968. H - *Lilyopsis fluoracantha*, slide J10, 20x. I - *Abylopsis tetragona*, slide U6, 20x. Slide metadata available in Dryad.

of these selected species were measured to capture intraspecific variation.

In order to observe the discharge behavior of different tentilla, we recorded high speed footage (1000-3000 fps) of tentillum and nematocyst discharge by live siphonophore specimens (26 species) using a Phantom Miro 320S camera mounted on a stereoscopic microscope. We mechanically elicited tentillum and nematocyst discharge using a fine metallic pin. We used the Phantom PCC software to analyze the footage. For the 10 species recorded, we measured total cnidoband discharge time (ms), heteroneme filament length (microns), and discharge speeds (mm/s) for cnidoband, heteronemes, haplonemes, and heteroneme shafts when possible (Appendix 4).

Siphonophore phylogeny – The phylogenetic analysis included 55 siphonophore species and 6 outgroup cnidarian species (*Clytia hemisphaerica*, *Hydra circumcincta*, *Ectopleura dumortieri*, *Porpita porpita*, *Vevelia velella*, *Staurocladia wellingtoni*). The gene sequences used in this study are available online (accession numbers in Appendix 5). Some of these sequences we used were accessioned in (Dunn et al. 2005), others we extracted from the transcriptomes in (Munro et al. 2018). Two new 16S sequences for *Frillagalma vityazi* (accession####) and *Thermopalia* sp. (accession####) analyzed by Lynne Christianson were included and accessioned to NCBI. We aligned these sequences using MAFFT (Katoh et al. 2002) (alignments available in Dryad). We inferred a Maximum Likelihood (ML) phylogeny (Appendix 6) from 16S and 18S ribosomal rRNA genes using IQTree (Nguyen et al. 2014) with 1000 bootstrap replicates (iqtree -s alignment.fa -nt AUTO -bb 1000). We used ModelFinder (Kalyaanamoorthy et al. 2017) implemented in IQTree v1.5.5. to assess relative model fit. ModelFinder selected GTR+R4 for having the lowest Bayesian Information Criterion score. Additionally, we inferred an Bayesian tree with each gene as an independent partition in RevBayes (Höhna et al. 2016) (Appendix 7, Appendix 9), which was topologically congruent with the unconstrained ML tree. The *alpha* priors were selected to minimize prior load in site variation.

Given the greater statistical power and credibility of the transcriptome phylogeny, we ran constrained inferences (using both ML and Bayesian timetree approaches, which produced congruent results (Appendix 6, Appendix 7)) fixing the 5 nodes that were incongruent with the topology of the consensus tree in (Munro et al. 2018). This tree was then used to inform a Bayesian relaxed molecular clock time-tree in RevBayes, using a birth-death process (sampling probability calculated from the known number of described siphonophore species) generating an ultrametric tree (Appendix 8). Scripts (Appendix 9) available in https://github.com/dunnlab/tentilla_morph/.

Feeding ecology – We extracted categorical diet data for different siphonophore species from published sources, including seminal papers (???, Biggs 1977; Purcell 1981, 1984; Andersen 1981; Pugh and Youngbluth 1988; Bardi and Marques 2007), and ROV observation data (Hissmann 2005; Choy et al. 2017) (Appendix 10). Since the sampling biases of ROV and gut content based methods are very different, the data were merged to the level of feeding guilds. The feeding guilds described here are: small-crustacean specialist (feeding mainly on copepods and ostracods), the large crustacean specialist (feeding on large decapods, mysids, or krill), the fish specialist (feeding mainly on actinopterygian larvae, juveniles, or adults), the gelatinous specialist (feeding mainly on other siphonophores, medusae, ctenophores, salps, and/or doliolids), and the generalist (feeding on a combination of the aforementioned taxa, without favoring any one prey group). We removed the gelatinous prey observations for *Praya dubia* eating a ctenophore and a hydromedusa and for *Nanomia* sp. eating *Aegina*, since we believe these are rare events that have a much larger probability of being detected by ROV methods than their usual prey, and it is not clear if the medusae were attempting to prey upon the siphonophores. Personal observations on feeding (from SHDH, CAC, and Philip Pugh) were also included for *Resomia ornicephala*, *Lychnagalma utricularia*, *Bargmannia amoena*, *Erenna richardi*, *Erenna laciniata*, *Erenna sirena*, and *Apolemia rubriversa*. We extracted copepod prey length data from (Purcell 1984). To calculate specific prey selectivities, we extracted quantitative diet and zooplankton composition data from (Purcell 1981), matched each diet assessment to each prey field quantification by site, calculated Ivlev's electivity indices (Jacobs 1974), and averaged those by species (Appendix 11).

Statistical analyses – For subsequent comparative analyses, we removed species present in the tree but not represented in the morphology data, and vice versa. Although we measured specimens labeled as *Nanomia bijuga* and *Nanomia cara*, we are not confident in some of the species-level identifications, and some specimens were missing diagnostic zooids. Thus, we decided to collapse these into a single taxonomic concept (*Nanomia* sp.). All *Nanomia* sp. observations were matched to the phylogenetic position of *Nanomia bijuga* in the tree. We carried out all phylogenetic comparative statistical analyses in the programming environment R (Team 2017), using the bayesian ultrametric species tree (Fig. 4), and incorporating intraspecific variation estimated

from the specimen data as standard error (Appendix 3). For each character (or character pair) analyzed, we removed species with missing data and reported the number of taxa included. We tested each character for normality using the Shapiro-Wilk test (Shapiro and Wilk 1965), and log-transformed those that were non-normal.

We fitted different models generating the observed data distribution given the phylogeny for each continuous character using the function `fitContinuous` (Harmon et al. 2007). The models compared were the white noise (WN) (non-phylogenetic model that assumes all values come from a single normal distribution with no covariance structure among species), the Brownian Motion (BM) model of neutral divergent evolution (Martins 1996), the Early Burst (EB) model of decreasing rate of evolutionary change (Harmon et al. 2010), and the Ornstein-Uhlenbeck (OU) model of stabilizing selection around a fitted optimum state (Uhlenbeck and Ornstein 1930; Butler and King 2004). We then ranked the models in order of increasing parametric complexity (WN,BM,EB,OU), and compared the corrected Akaike Information Criterion (AICc) support scores (Sugiura 1978) to the lowest (best) score, using a cutoff of 2 units to determine significantly better support. When the best fitting model was not significantly better than a less complex alternative, we selected the least complex model (Appendix 12). We calculated model adequacy scores using the R package `arbutus` (Pennell et al. 2015) (Appendix 13). We calculated phylogenetic signal in each of the measured characters using Blomberg's K (Blomberg et al. 2003) (Appendix 12), and for the morphological dataset as a whole using the R package `geomorph` (Adams et al. 2016). We reconstructed ancestral states using Maximum Likelihood (`anc.ML` (Revell 2012)), and stochastic character mapping (`make.simmap`) for categorical characters. R scripts available in Dryad.

In order to study the evolution of predatory specialization, we reconstructed components of the diet and prey selectivity on the phylogeny using ML (R `phytools::anc.ML`). To identify evolutionary associations of diet with tentillum and nematocyst characters, we compared the performance of a neutral evolution model to that of a diet-driven directional selection model. First, we collapsed the diet data into five feeding guilds (fish specialist, small crustacean specialist, large crustacean specialist, gelatinous specialist, generalist), based on which prey types they were observed consuming most frequently. We reconstructed the feeding guild ancestral states using the ML function `ace` (package `ape` (Paradis et al. 2019)), removing tips with no feeding data. The ML reconstruction was congruent with the consensus stochastic character mapping (Appendix 18). Then, using the package `OUwie` (Beaulieu and O'Meara 2012), we fitted an OU model with multiple optima and rates of evolution matched to the reconstructed ancestral diet regimes, a single optimum OU model, and a BM null model. Finally, we compared their AICc support values to select the best fitting model (Appendix 14).

To model the relationships between individual tentillum and nematocyst characters and the ability to capture particular prey types in the diet, we ran a series of phylogenetic generalized linear models (R `phytools::phyloglm`) (Appendix 17). In addition, we ran a series of comparative analyses to address hypotheses of diet-tentillum relationships posed in the literature. To test for correlated evolution among binary characters, we used Pagel's test (Pagel 1994). To characterize and evaluate the relationship between continuous characters, we used phylogenetic generalized least squares regressions (PGLS) (Grafen 1989). To compare the evolution of continuous characters with categorical aspects of the diet, we carried out a phylogenetic logistic regression (R `nlme::gls`).

To identify the morphological characters with the greatest ability to diagnose and predict diet, we carried out linear discriminant analysis of principal components (DAPC) using the `dapc` function (R `adegenet::dapc`) (Jombart et al. 2010). We generated discriminant functions for feeding guild, presence of copepods, fish, and shrimp (large crustaceans) in the diet (Appendix 15). For these specific groups, we then generated and compared generalized linear models (GLMs) with multiple predictors. We chose predictors among the characters with significant loading contributions in each specific DAPC. We then selected the best GLM for each prey type based on the lowest AIC scores.

In order to explore the correlational structure among continuous characters and among their evolutionary histories, we used principal component analysis (PCA) and phylogenetic PCA (Revell 2012). Since the character data contains many gaps due to missing characters, we carried out these analyses on a subset of species and characters that allowed the largest data volume. In addition, we obtained the correlations between the phylogenetic independent contrasts (Felsenstein 1985) using the package `rphylip` (Revell and Chamberlain 2014).

To test how many times extreme nematocyst morphologies evolved, we reconstructed the ancestral states

of $\log(\text{length}/\text{width})$ of the different nematocyst types, and identified the branches with the greatest shifts. In addition, we ran a Bayesian Analysis of Macroevolutionary Mixtures (BAMM) (Rabosky et al. 2014) on haploneme and heteroneme elongation to estimate the number and phylogenetic mapping of trait evolution rate regimes (Appendix 16).

Results

Phylogeny – Only 5 nodes in the unconstrained inference were incongruent with the (Munro et al. 2018) transcriptome tree. The topology of the constrained tree presented here (Fig. 4) is congruent with the resolved nodes in (Dunn et al. 2005) and (Munro et al. 2018).

We define two new clades within Codonophora (Fig. 4): Eucladophora as the clade containing *Agalma elegans* and all taxa that are more closely related to it than to *Apolemia lanosa*, and Tendiculophora as the clade containing *Agalma elegans* and all taxa more closely related to it than to *Bargmannia elongata*. Eucladophora is characterized by bearing spatially differentiated tentilla with proximal heteronemes and a narrower terminal filament region. The etymology derives from the Greek for “true branch bearers”. Tendiculophora are characterized by bearing rhopalonemes and desmonemes in the terminal filament, having a pair of elastic strands, and developing proximally detachable cnidobands. The etymology of this clade is derived from the Latin tendicula for “snare or noose”.

Evolutionary dynamics between diet and tentillum morphology – The reconstructions of feeding guilds show that generalism was not likely ancestral, and it appears to have evolved at least 2 times independently (Fig. 5). Individual prey type presence reconstructions show that copepod specialization and fish specialization evolved twice, ostracod specialization evolved at least once. The OUwie model comparison shows that out of 30 characters, 10 show significantly stronger support for the diet-driven multi-optima multi-rate OU model (Appendix 14). These characters include terminal filament nematocyst size and shape, involucrum length, elastic strand width, and heteroneme number. Most of these characters are found exclusively in Tendiculophora, thus this reflects processes that could be unique to this subtree. Five characters including cnidoband length, cnidoband shape, and haploneme length show maximal support for a diet-driven single-optimum OU model. The remaining 15 characters support BM (or OU with marginal AICc difference with BM).

Phylogenetic logistic regressions identified evolutionary associations between individual characters and the presence of particular prey types in the diet (Fig. @??figure5, right). Shifts toward ostracod presence in diet correlated with reductions in pedicle width and total haploneme volume. Shifts to copepod presence in the diet were associated with reductions in haploneme width, cnidoband length and width, total haploneme and heteroneme volumes, and tentacle and pedicle widths. Consistently, transitions to decapod presence in the diet correlated with more coiled cnidobands (Appendix 17).

Phylogenetic regressions of continuous characters against prey selectivity data produced additional insights. Specialization in a piscivorous diet was associated with increased number of heteronemes per tentillum, increased roundness of nematocysts (desmonemes and haplonemes), larger heteronemes, reduced heteroneme/cnidoband length ratios, smaller rhopalonemes, lower haploneme SA/V ratios, and increased size of the cnidoband, elastic strand, pedicle and tentacle widths. Decapod-rich diets were associated with increasing cnidoband size and coiledness, haploneme row number, elastic strand width, and heteroneme number. Copepod-selective diets evolved in association with smaller heteroneme and total nematocyst volumes, smaller cnidobands, rounder rhopalonemes, elongated heteronemes, narrower haplonemes with higher SA/V ratios, and smaller heteronemes, tentacles, pedicles and elastic strands. Selectivity for ostracods was associated with reductions in size and number of heteroneme nematocysts, reductions in cnidoband size, number of haploneme rows, heteroneme number, and cnidoband coiledness. Heteroneme length and shape also correlated negatively with chaetognath selectivity.

When some of the diet-morphology associations reported in the literature (Purcell 1984; Purcell and Mills 1988) were tested for correlated evolution (Table 1), we found that most were consistent with an evolutionary explanation except the relationship between terminal filament nematocysts (rhopalonemes and desmonemes) and crustaceans in the diet. The latter is likely a product of the larger species richness of crustacean eating species with terminal filament nematocysts, rather than simultaneous evolutionary gains.

Tentilla morphology as a predictor of siphonophore diet and prey selectivity – The discriminant analysis of principal components for feeding guild produced 86% discrimination (Appendix 15), and significant loadings

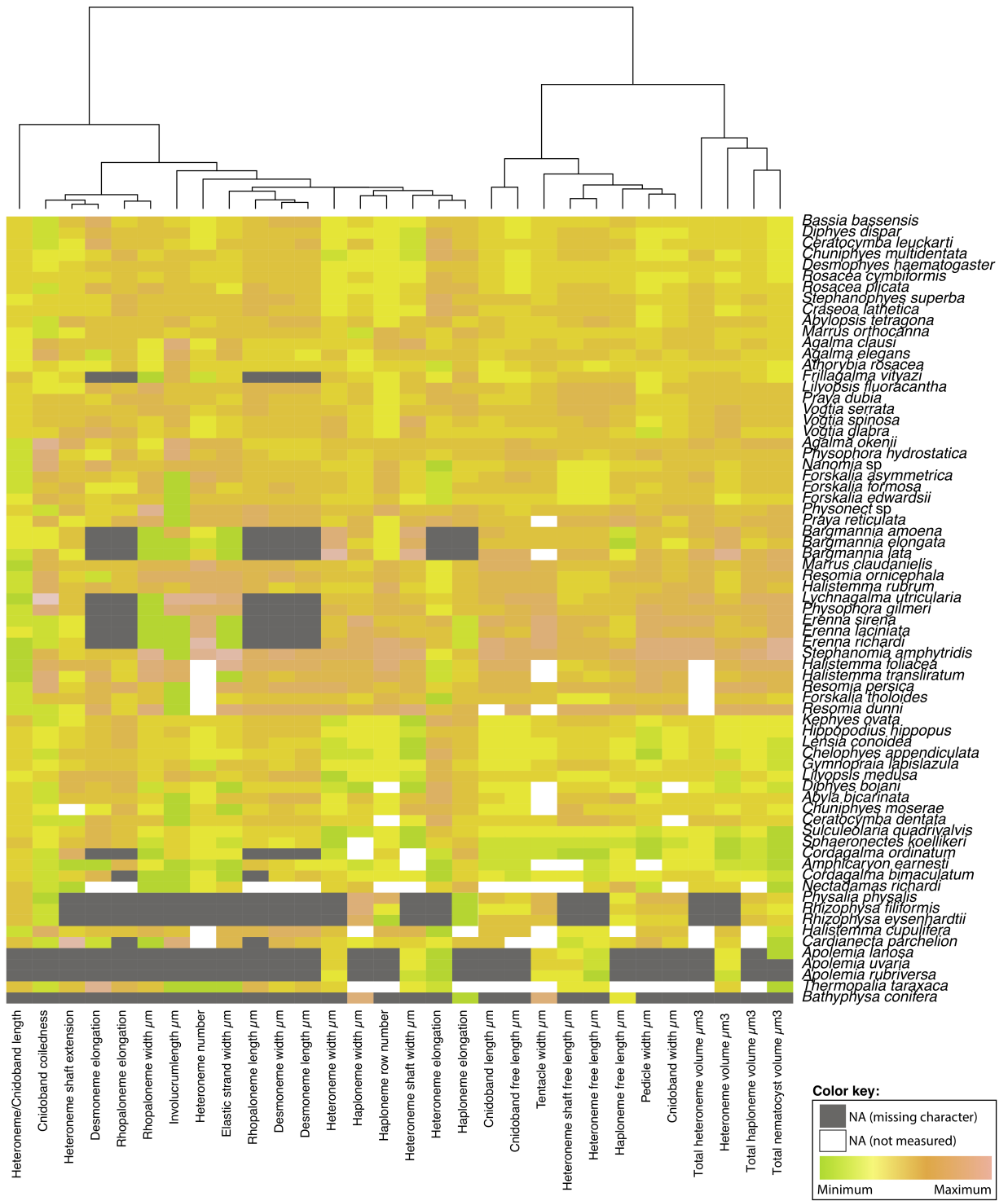


Figure 3: Heatmap summarizing the morphological diversity measured for 96 species of siphonophores (raw data in Appendix 3). Missing values from absent characters presented as dark grey cells, missing values produced from technical difficulties presented as white cells. Values scaled by character.

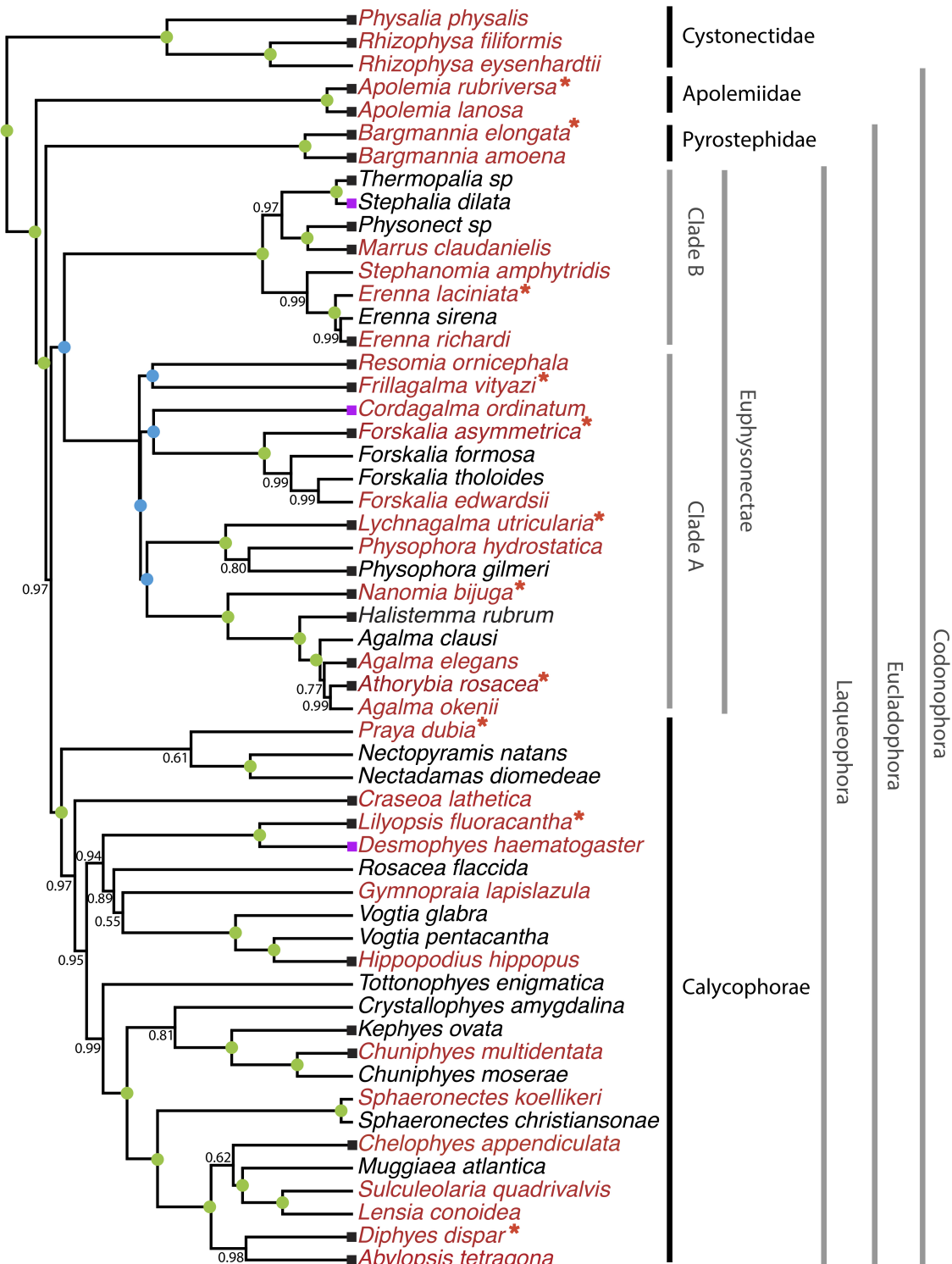


Figure 4: Bayesian time-tree built from 18S + 16S concatenate. Branch lengths estimated using relaxed molecular clock. Species names in red indicate replicated representation in the morphology data. Species marked with an asterisk were recorded using high speed video. Nodes labeled with bayesian posteriors (BP). Green circles indicate BP = 1. Blue circles indicate nodes constrained to be congruent with (Munro *et al.* 2018). Tips with black squares indicate the species with transcriptomes used in (Munro *et al.* 2018). Tips with grey squares indicate genus-level correspondence to taxa included in (Munro *et al.* 2018). The main clades are labeled: in black for described taxonomic units, and in grey for operation phylogenetic designations.

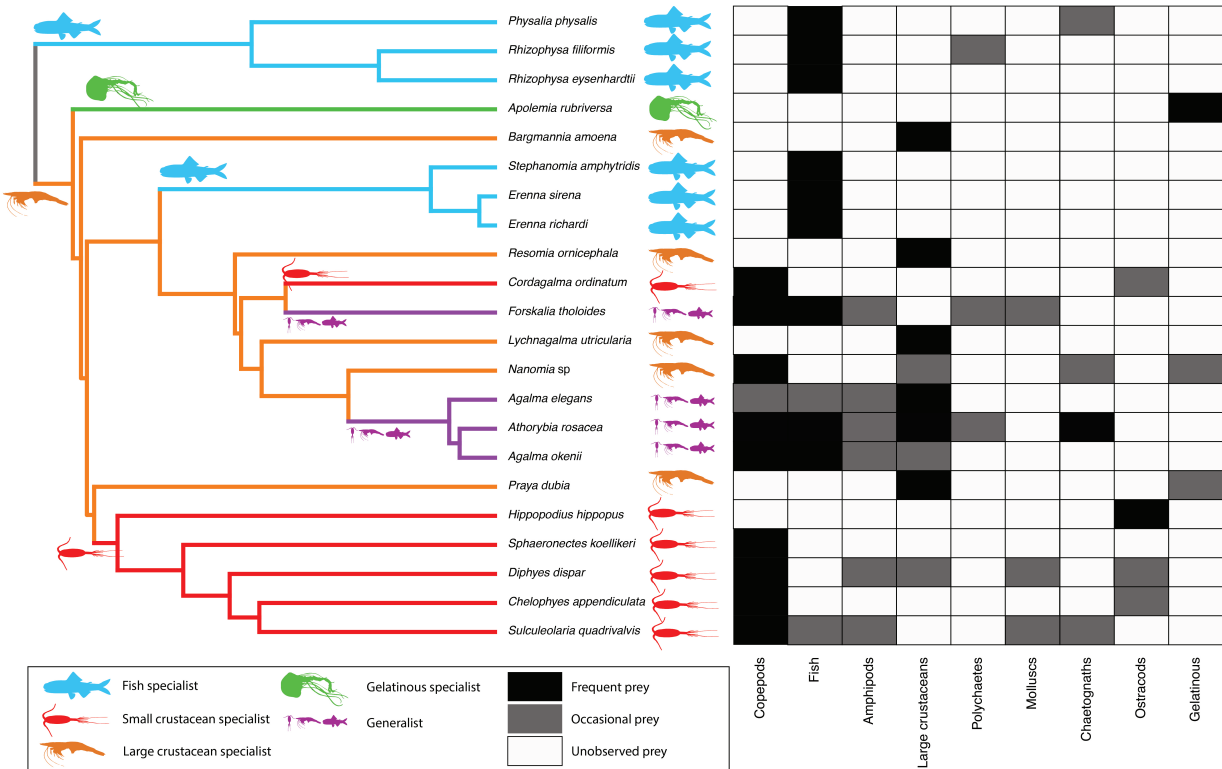


Figure 5: Left - Subset phylogeny showing the mapped feeding guild regimes that were used to inform the OUwie analyses. Right - Grid showing the prey items consumed from which the feeding guild categories were derived. Diet data were obtained from the literature review in Appendix 10.

Character	Aspect of diet	Test of evolutionary association	Relationship sign	P-value	Number of taxa	Association first report
Differentiated cnidobands	Hard bodied prey	Pagel's test	+	0.017	19	Purcell, 1984
Heteroneme volume	Copepod prey size	pGLS	+	0.002	8	Purcell, 1984
Terminal filament nematocysts	Crustacean diet	Pagel's test	+	0.2	19	Purcell & Mills, 1988
Number of nematocyst types	Soft-bodied prey	Phylogenetic logistic regression	-	0.04	22	Purcell & Mills, 1988

Figure 6: Tests of correlated evolution between morphological characters and aspects of the diet found correlated in the literature.

were found for the characters (ordered from highest to lowest): Heteroneme size, involucrum length, total haploneme and heteroneme volume, cnidoband length, heteroneme/cnidoband length ratio, heteroneme width, and cnidoband length and width. The only groups confounded were large crustacean specialists and generalists. For this analysis, we transformed the missing values in the data (due to character absence) to zeroes, thus accommodating more taxa and characters.

We used this discriminant function to predict the feeding guild of 45 species in our morphological data (Fig. 7). When predicting soft and hard bodies prey specialization, the DAPC achieves 90.9% discrimination success, only marginally confounding hard-bodied specialists with generalists (Appendix 15). The main characters driving the discrimination are cnidoband coiledness, cnidoband length, tentacle width, haploneme elongation, and cnidoband width. Discriminant analyses and GLM were also applied to specific prey type presence and selectivity (Table 8, highlighting the most relevant characters and their predictive power).

Evolution of tentillum and nematocyst characters – One third of the characters measured support a non-phylogenetic generative model, indicating they are more stochastically than phylogenetically distributed (Appendix 12). Total nematocyst volume and cnidoband-to-heteroneme length ratio showed strongly conserved phylogenetic signals. 74% of characters present a significant phylogenetic signal, yet only total nematocyst volume, haploneme length, and heteroneme to cnidoband length ratio had a phylogenetic signal $K > 1$. 67% of characters support BM models, indicating a history of neutral constant divergence. No relationship between phylogenetic signal and BM model support was found. Haploneme nematocyst length is the only character with support for an EB model of decreasing rate of evolution with time. No character had support for a single-optimum OU model.

The phylogenetic positions of the main categorical character shifts were reconstructed with stochastic character mappings (Appendix 18), and summarized in Figure 9. Haploneme nematocysts are likely ancestrally present in the tentacles, since they are present in the tentacles of many other hydrozoans. Haplonemes diverged into spherical isorhizas of 2 size classes in Cystonectae, and elongated anisorhizas of one size class in Codonophora. Haplonemes were likely lost in the tentacles of *Apolemia*, but spherical isorhizas are retained in other *Apolemia* tissues (Siebert et al. 2013). Similarly, while heteronemes exist in other tissues of cystonects, they only appear in the tentacles of codonophorans as birhopaloids in *Apolemia*, ancestral stenoteles in eucladophoran physonects, and microbasic mastigophores in calycophorans.

Eucladophora (the clade containing Pyrostephidae, Euphysonectae, and Calycophorae, see Fig. 4) encompasses most of the extant Siphonophore species. Innovations evolved in the stem of this group include spatially segregated heteroneme and haploneme nematocysts, terminal filaments, and elastic strands (Fig. 9). Pyrostephids evolved a unique bifurcation of the axial gastrovascular canal of the tentillum known as the “saccus” (Totton and Bargmann 1965). The stem to the clade Tendiculophora (clade containing Euphysonectae and Calycophorae, see Fig. 4) subsequently acquired further novelties such as the desmoneme and rhopaloneme (acrophore type ancestral) nematocysts on the terminal filament (Fig. 9), which would bear no other nematocyst type, and these would be arranged in sets of 2 parallel rhopalonemes for each single desmoneme (Skaer 1988, 1991). The involucrum is an expansion of the epidermal layer that can cover part or all of the cnidoband. This structure, together with differentiated larval tentilla, appeared in the stem branch to Clade A physonects. Calycophorans evolved unique novelties such as larger desmonemes at the distal end of the cnidoband, pleated pedicles with a “hood” (here considered homologous to the involucrum) at the proximal end of the tentillum, anacrophore rhopalonemes, and microbasic mastigophore type heteronemes.

Phenotypic integration of the tentillum – The quantitative characters we measured from tentilla and their nematocysts are very correlated to each other. Of the phylogenetic correlations (Fig. 8a, lower triangle), 81.3% were positive and 18.7% were negative, while of the ordinary correlations (Fig. 10a, upper triangle) 74.6% were positive and 25.4% were negative. Half (49.9%) of phylogenetic correlations were >0.5 , while only 3.6% are < -0.5 . Similarly, of the across-species correlations, 49.1% were >0.5 and only 1.5% were < -0.5 . 13.9% of character pairs had opposing phylogenetic and ordinary correlation coefficients. Just 4% have negative phylogenetic and positive ordinary correlations, and vice versa for 9.9% of character pairs. These disparities can be caused by Simpson’s paradox (Blyth 1972), the reversal of the sign of a relationship when a third variable (or a phylogenetic topology (Uyeda et al. 2018)) is considered. However, no character pair had correlation coefficient differences larger than 0.74 between ordinary and phylogenetic correlations.

In the raw (non-morphometric) PCA morphospace (Fig. 11), PC1 (aligned with tentillum and tentacle size) explains 69.3% of the variation in the tentillum morphospace, whereas PC2 (aligned with heteroneme length, heteroneme number, and haploneme arrangement) explained 13.5%. In a phylogenetic PCA, 63% of

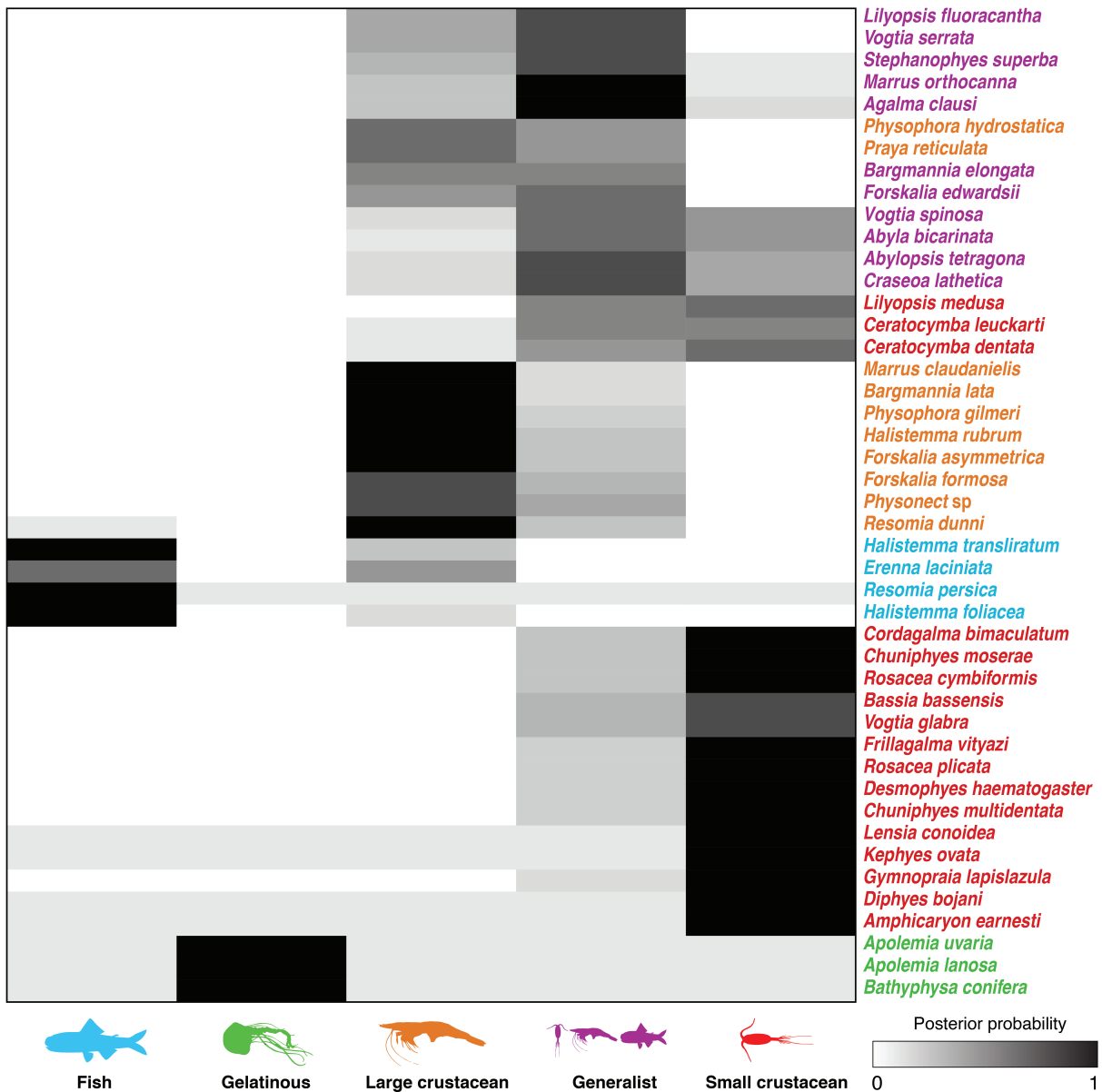


Figure 7: DAPC predicted feeding guilds for siphonophore species with measured tentilla morphology data but without any preliminary dietary data. Cell darkness indicates posterior probability of belonging to each guild. Training data set transformed so missing values would be computed as zeroes. Species colored according to their predicted feeding guild with highest probability score.

Prey type	DAPC		Best fitting GLM for prey type presence (22 taxa)			Best fitting GLM for prey type selectivity (Purcell, 1981) (7 taxa)		
	Discrimination (%)	Significant loadings	Predictors	Sign	Pseudo-R ²	Predictors	Sign	Pseudo-R ²
Copepods	100	Tentacle width	Tentacle width	-	76.3	Tentacle width	-	76.6
		Haploneme row number	Haploneme row number	-		Haploneme row number	-	
		Total haploneme volume				Total haploneme volume	-	
		Haploneme width						
		Haploneme surface area/volume ratio						
Fish	63	Heteroneme volume	Heteroneme volume	+	36.7	Pedicle width	+	97.5
		Total haploneme volume	Total haploneme volume	-				
		Pedicle width	Pedicle width	+				
		Heteroneme elongation						
		Heteroneme width						
Large crustaceans	100	Heteroneme volume	Heteroneme volume	+	85.6	Heteroneme volume	+	89.1
		Cnidoband coiledness	Cnidoband coiledness	+		Cnidoband coiledness	+	
		Cnidoband length	Cnidoband length	-		Cnidoband length	-	
		Haploneme elongation	Haploneme elongation	+		Haploneme elongation	+	
		Heteroneme elongation	Heteroneme elongation	-		Heteroneme elongation	-	

Figure 8: Discriminant analysis of principal components for specific prey types using the morphological data. Loadings are ordered from highest to lowest significance. GLMs were fitted to predict prey type presence and selectivity for different combinations of the significant loadings and selected for the lowest AIC value. Only the best GLM is reported. Pseudo-R² approximate the variance explained by the model.

the evolutionary variation in the morphospace is explained by PC1 (aligned with shifts in tentillum size), while 18% is explained by PC2 (aligned with shifts in heteroneme number and involucrum length). These results indicate that the dimensionality of tentillum morphology is low, that many traits are associated with size, but that nematocyst arrangement is independent of it.

Evolution of nematocyst shape – Haploneme nematocyst evolution has been mainly driven by a single large shift towards elongation in Tendiculophora, which contains the majority of described siphonophore species. There is one secondary return to more oval, less elongated haplonemes in *Erenna*, but it doesn't reach the sphericity present in Cystonectae or Pyrostephidae (Fig. 12). Heteroneme evolution presents a less radical evolutionary history, where Tendiculophora evolved more elongate heteronemes, but the difference between theirs and other siphonophores is much smaller than the variation in shape within Tendiculophora, bearing no phylogenetic signal. In this group, evolution of heteroneme shape has diverged in both directions, and there is no correlation with haploneme shape, which has remained fairly constant (elongation between 1.5 and 2.5).

Haploneme and heteroneme shape share 21% of their variance across extant values, and 53% of variance in their shifts alongs the branches of the phylogeny. However, much of this correlation is due to the contrast between pyrostephids and its sister group. BAMM identified a regime shift in heteroneme shape evolution on the branches leading to *Agalma* and *Athorybia*. For the rates of haploneme shape evolution, BAMM identified two main independent regime shifts (Fig. 12): one in the branch leading to Codonophora (anisorhizas diverging from cystonects' spherical isorhizas), and one in the branch leading to Clade B physonects (most have rod-shaped anisorhizas, but *Erenna* has oval ones). No clear patterns were identified in the evolution of desmoneme and rhopaloneme shape.

Functional morphology of tentillum and nematocyst discharge – While the sample sizes of high speed measurements were insufficient to draw reliable statistical results at a phylogenetic level, we did observe patterns that may be relevant to their functional morphology. For example, cnidoband length is strongly correlated with discharge speed (p value = 0.0002). This is probably the sole driver of the considerable difference between euphysonect and calycophoran tentilla discharge speeds (average discharge speeds: 225.0mm/s and 41.8mm/s respectively. T-test p value = 0.011), since the euphysonects have larger tentilla than the calycophorans among the species recorded.

We also observed that calycophoran haploneme tubules fire faster than those of euphysonects (T-test p value = 0.001). Haploneme nematocysts discharge 2.8x faster than heteroneme nematocysts (T-test p value = 0.0012). Finally, we observed that the stenoteles of the Euphysonectae discharge a helical filament that “drills” itself through the medium it penetrates as it everts.

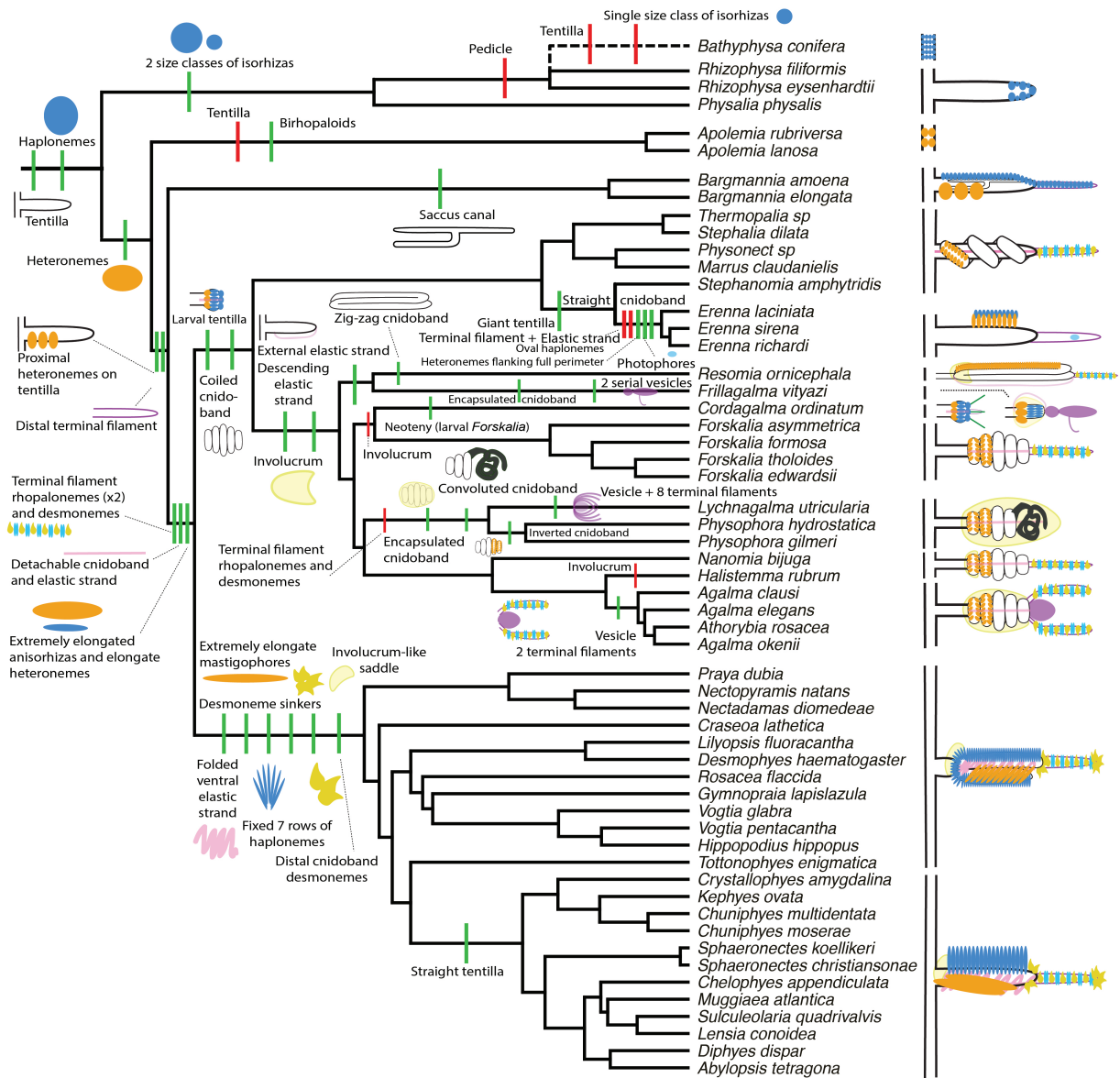


Figure 9: Bayesian cladogram with the main categorical character gains (green) and losses (red) mapped. The main visually distinguishable tentillum types are sketched next to the species that bear them, showing the location and arrangement of the main characters. In large complex-shaped tentilla, haplonemes were omitted for simplification. The rhizophysid *Bathyphysa conifera* branch was appended manually as a polytomy (dashed line).

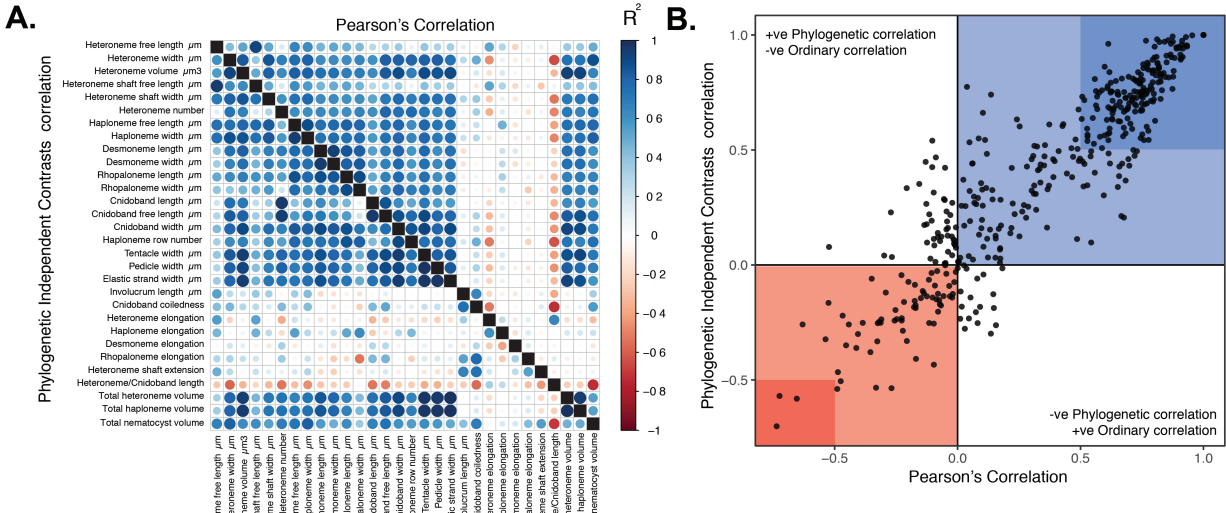


Figure 10: A. Correlogram showing strength of ordinary (upper triangle) and phylogenetic (lower triangle) correlations between characters. Both size and color of the circles indicate the strength of the correlation (R^2). B. Scatterplot of phylogenetic correlation against ordinary correlation showing a strong linear relationship ($R^2 = 0.92$, 95% confidence between 0.90 and 0.93). Light red and blue boxes indicate congruent negative and positive correlations respectively. Darker red and blue boxes indicate strong (<-0.5 or >0.5) negative and positive correlation coefficients respectively.

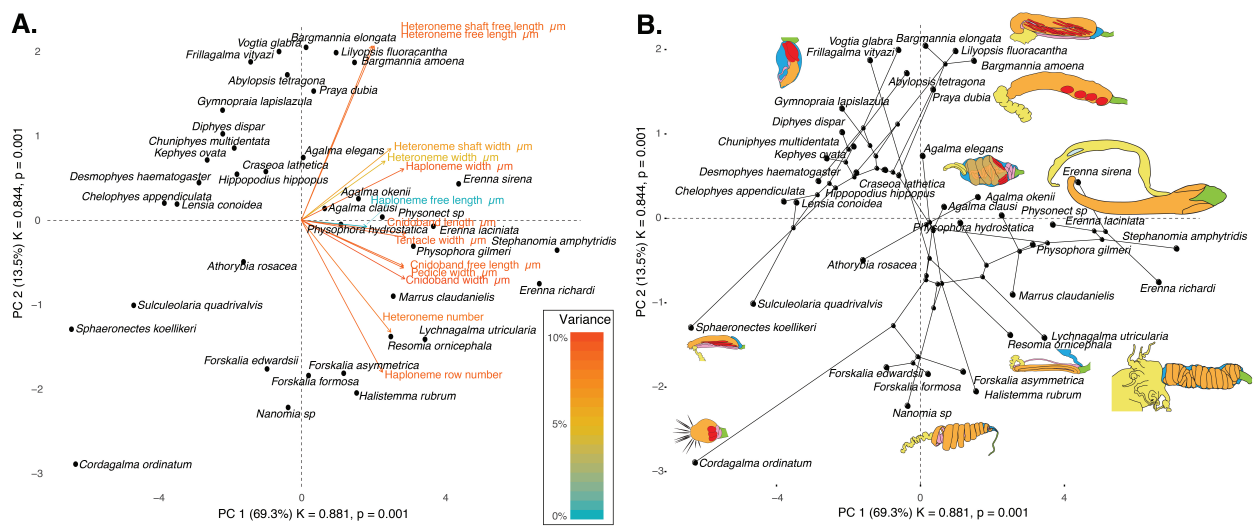


Figure 11: Phylomorphospace of the simple continuous characters principal components, excluding ratios and composite characters. A. Variance explained by each variable in the PC1-PC2 plane. Axis labels include the phylogenetic signal (K) for each component and p-value. B. Phylogenetic relationships between the species points distributed in that same space.

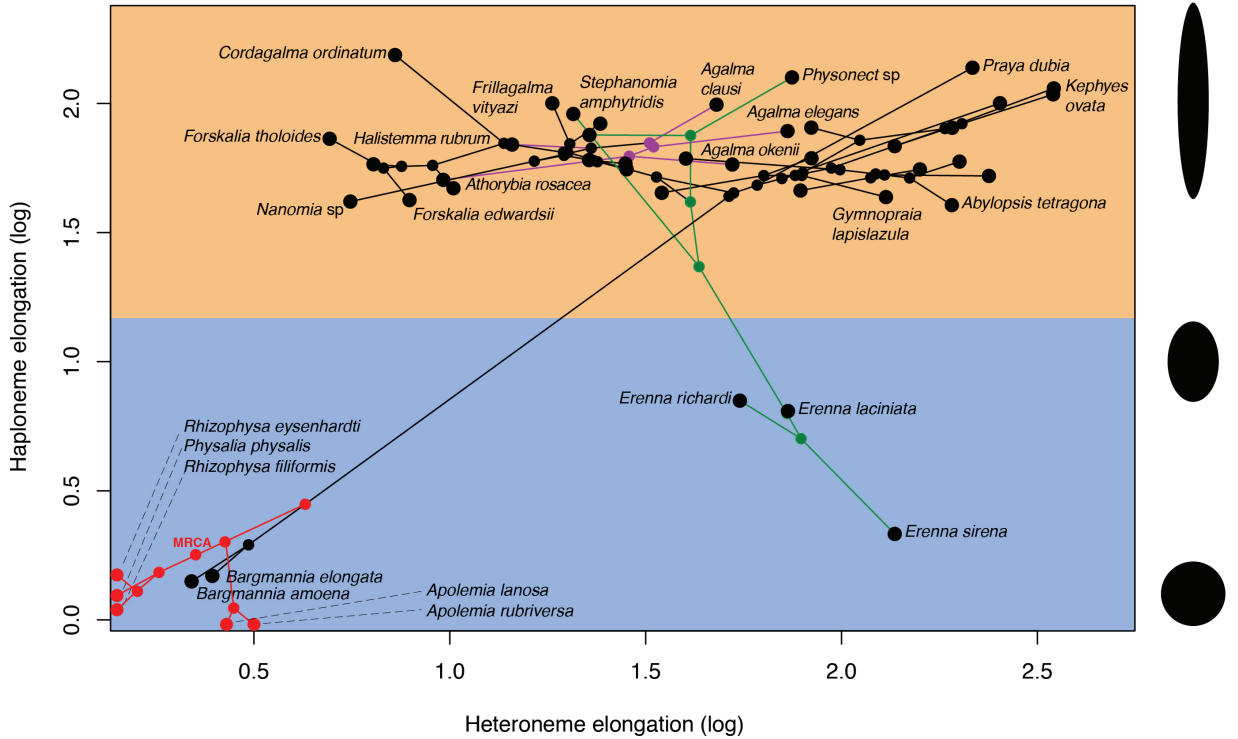


Figure 12: Phylomorphospace showing haploneme and heteroneme elongation (log scaled). Orange area delimits rod-shaped haplonemes, blue area covers oval and round shaped haplonemes. Smaller dots and lines represent phylogenetic relationships and ancestral states of internal nodes under BM. Species nodes in red were manually added to the plot. Cystonects have no tentacle heteronemes and are projected onto the haploneme axis. Apolemids have no tentacle haplonemes and are project onto the heteroneme axis. Colored branches and nodes correspond to BAMM regimes of accelerated haploneme shape (green) and heteroneme shape (violet) evolution.

Discussion

This core aim of this paper is to characterize the evolutionary history of siphonophore tentilla and its relationships with diet. In addition, we produced novel findings on tentilla morphology, siphonophore phylogeny, nematocyst character evolution, and tentillum discharge dynamics.

Evolution of tentilla morphology with diet – Siphonophores are an abundant group of zooplankton in oceanic ecosystems (Longhurst 1985; O'Brien 2007). While little is known about siphonophore trophic ecology, what is known indicates that they occupy a central position in midwater food webs (Choy et al. 2017), potentially serving as trophic intermediaries between smaller zooplankton and higher trophic level predators. Siphonophore species have been observed to feed on a variety of prey with very different sizes, traits, and behaviors. With a total absence of siphonophores in the fossil record, how they became established as the ubiquitous and diversified predators in today's oceans remains an open question. Predators that use similar tools for prey capture tend to capture similar prey, so their abundance and coexisting species diversity trade-off through competition (Schluter 2000). However, this is not consistent with what we observe in siphonophores, which have been found to be both very abundant and locally diverse (Longhurst 1985, Mapstone (2014)). We hypothesize that siphonophores have escaped this trade-off through specialization on different prey resources.

The evolutionary history of tentilla shows that siphonophores are an example of ecological niche diversification via morphological innovation and evolution. This strategy is particularly important in open ocean ecosystems, a homogeneous abiotic environment where the only niche heterogeneity available is the potential interactions between organisms (Robison 2004).

The evolutionary history of siphonophore diets indicates that being a specialist was an ancestral aspect of their trophic niche, while trophic generalism is likely a derived condition. Several studies (reviewed in (Futuyma and Moreno 1988)) have suggested that resource specialization is an irreversible dead end due to the constraints posed by their phenotypic specialization. Our reconstructions show that this is not the case for siphonophores, where the prey type on which they specialize has shifted at least 5 times, and generalism has evolved independently at least twice.

An increase in clade richness and ecological diversification can be triggered by a 'key innovation' (Simpson 1955). The evolutionary innovation of the Tendiculophora tentilla with shooting cnidobands and modular regions may have facilitated further dietary diversification to unfold.

Throughout this study, we evaluate our findings from an adaptive perspective, assessing whether our results are congruent with adaptation. However, our analyses are not sufficient to adequately test hypotheses of adaptation, since that would require evidence of changes within a population exposed to different selective pressures.

One of the most common prey items found in siphonophore diets are copepods (Fig. 5). Copepod-specialized diets have evolved convergently in *Cordagalma* and some Calycophorans. These evolutionary transitions happened together with transitions to smaller tentilla with fewer cnidoband nematocysts. Tentilla are expensive single-use structures, therefore we would expect that specialization in small prey would beget reductions in the size of the prey capture apparatus to the minimum required for the ecological function. *Cordagalma*'s tentilla strongly resemble the larval tentilla (only found in the first-budded feeding body of the colony) of their sister genus *Forskalia* spp. This indicates that the evolution of *Cordagalma* tentilla could be a case of paedomorphosis associated with predatory specialization.

(Purcell 1984) showed that haplonemes have a penetrating function as isorhizas in cystonects and an adhesive function as anisorhizas in Tendiculophora. The two clades that have been observed primarily feeding on fish (Cystonectae and Clade B) present an accelerated rate of haploneme shape evolution towards more compact haplonemes, significantly distinct from their closest relatives. Isorhizas in cystonects are known to penetrate the skin of fish during prey capture, and to deliver the toxins that aid in paralysis and digestion (Hessinger 1988). *Erenna* anisorhizas are also able to penetrate human skin and deliver a painful sting (Pugh 2001), a common feature of piscivorous cnidarians like cystonects or cubozoans.

(Thomason 1988) hypothesized that smaller, more spherical nematocysts, with a lower surface area to volume ratio, are more efficient in osmotic-driven discharge and thus have more power for skin penetration. The elongated haplonemes of crustacean-eating Tendiculophora have never been observed penetrating their crustacean prey ((Purcell 1984) and personal observations), and are hypothesized to entangle the prey through adhesion of the abundant spines to the exoskeletal surfaces and appendages. Entangling requires

less acceleration and power during discharge than penetration, as it does not rely on point pressure. In fish-eating cystonects and erennids, the haplonemes are much less elongated and very effective at penetration, in congruence with the osmotic discharge hypothesis. The accelerated rate of heteroneme shape evolution in the clade containing *Agalma* and *Nanomia* may indicate a rapid dietary differentiation. However, our limited ecological data does not show any significant dietary differentiation in this group.

When the diet-morphology correlation hypotheses supported in the literature were tested from a macroevolutionary perspective, we found that most of them were consistent with correlated evolution (Table 2). The ecomorphological association between rhopalonemes, desmonemes and crustacean eaters was not congruent with a scenario of correlated evolution. This could be due to our analysis with a broad set of taxa including multiple species without desmonemes or rhopalonemes that effectively capture crustaceans (such as *Cordagalma ordinatum*, *Lychnagalma utricularia*, and *Bargmannia amoena*).

While our results unambiguously show that tentilla morphology evolved with diet, the conclusions we can draw from these analyses are limited by the sparse dietary data available. In addition, diet is a product of environmental prey availability and predator selectivity. Selectivity differences across siphonophore species could be driven by other phenotypes not accounted for this study. For example, tentacle deploying behavior, positioning in the water column, or behavioral decisions on whether or not to discharge on or ingest an encountered animal. Further observations on these behaviors in the field are necessary to assess their relative importance in determining dietary composition. In addition to behavior, there is much biochemistry in the prey capture and digestion processes that remains unexplored. Part of the success in siphonophore prey capture is likely determined by the effectivity of the toxins delivered by the nematocysts on different taxa. Comparative toxin assays, and venom protein evolution studies could shed light on this question. Moreover, siphonophore trophic specialization may have brought changes in the digestive biochemistry of gastrozooids and palpons. A comparison of the gene expression levels for different enzymes in the gastrozooids of different species, together with digestive enzyme sequence evolution studies, and a toxicological assay of the different venoms in siphonophore nematocysts on different prey taxa, would provide a great complement to our results.

Predicting siphonophore feeding ecology – One motivation for our research was to understand the links between predator capture tools and their diets so we can better predict the diets of siphonophores based on morphological characteristics. Our discriminant analyses were able to distinguish between different siphonophore diets based on morphological characters alone. The models produced by these analyses generated untested predictions about the diets of many species for which we only have morphological data of their tentacles. In future work, we can test these ecological hypotheses and validate these models by directly characterizing the diets of some of those siphonophore species. Predicting diet using morphology is a powerful tool to reconstruct food web topologies from community composition alone. Interactions among the oceanic zooplankton have been treated as a black box in ecological models (Mitra 2009). The ability to predict such interactions, including those of siphonophores and their prey, will enhance the taxonomic resolution of nutrient flow models from plankton trawl data.

Phenotypic integration of siphonophore tentilla – Tentillum characters, such as nematocysts, arose from the subfunctionalization of serial homologs (David et al. 2008). Serial homologs have shared genetic elements underlying their development, and are expected to have phylogenetic correlations. In addition, these substructures must fit and work together in synchrony to ensnare prey successfully (functional integration). Character complexes that satisfy these conditions tend to be phenotypically integrated. Phenotypic integration is the set of functional and genetic correlations among the traits of an organism (Pigliucci 2003). These correlations have been hypothesized to direct and constrain adaptive evolution (Wagner and Schwenk 2000). The siphonophore tentillum morphospace has a fairly low extant dimensionality due to an evolutionary history with many synchronous, correlated changes. This is consistent with strong phenotypic integration where genetic and developmental correlations are maintained by natural selection to preserve function.

Part of the tentillum structural correlations are to be expected from shared regulatory networks for elements that develop together from common positional bud (budding tentilla in the tentacle). Similarly, correlations between nematocyst subtypes are also expected given their common evolutionary and developmental origin. None of these explanations for correlated evolution are surprising, nor require natural selection. However, we also found correlations between nematocyst and tentillum characters. Siphonophore tentacle nematocysts (in their cnidocytes) are not produced nor matured in the developing tentillum. These cnidocytes are produced by dividing cnidoblasts in the basigaster (basal swelling of the gastrozooid). Once the cnidocytes have assembled the nematocyst, they migrate up the tentacle (Carré 1972) and position themselves in the tentillum

according to their type and size (Skaer 1988). Thus, the developmental programs that produce the observed nematocyst morphologies are spatially separated from those producing the tentilla morphologies. Therefore, we hypothesize the genetic correlations and phenotypic integration between tentillum and nematocyst characters is maintained through natural selection on separate regulatory networks, out of the necessity to work together and meet the spatial, mechanical, and functional constraints of their prey capture behavior.

Evolutionary history of tentilla morphology – This study produced the most speciose siphonophore molecular phylogeny to date, while incorporating the most recent findings in siphonophore deep node relationships. This revealed for the first time that *Erenna* is the sister to *Stephanomia amphytridis*. *Erenna* and *Stephanomia* bear the largest tentilla among all siphonophores, thus their monophyly indicates that there was a single evolutionary transition to giant tentilla.

Tentillum size, as well as the majority of the characters studied, supported BM evolutionary models. There are two alternative hypotheses about the generative process of BM. One hypothesis would suggest that these characters are not under selection, and therefore diverging neutrally (Lande 1976). The second hypothesis suggests that they are under selection, however, the adaptive landscape was rapidly shifting (Hansen and Martins 1996), without leaving clear patterns on the phylogeny. Some of the BM supported characters are likely to have evolved under the second hypothesis, for when a diet (feeding guild) driven regime tree was provided, these characters preferentially supported an OU model (Appendix 14).

Siphonophore tentilla are defined as lateral, monostichous evaginations of the tentacle gastrovascular lumen with epidermal nematocysts (Totton and Bargmann 1965). The buttons on *Physalia* tentacles were not traditionally regarded as tentilla, but (Bardi and Marques 2007) and our observations (Munro et al. 2018), confirm that the buttons contain evaginations of the gastrovascular lumen, thus satisfying all the criteria for the definition. In this light, and given that most Cystonectae bear conspicuous tentilla, we conclude (in agreement with (Munro et al. 2018)) that tentilla are likely ancestral to all siphonophores, and secondarily lost in *Apolemia* and *Bathyphysa conifera*.

A clear example of convergent evolution we found, is that the calycophoran tentillum morphospace (Fig. 11) was secondarily occupied by *Frillagalma vityazi*. Like calycophorans, *Frillagalma* tentilla have small C-shaped cnidobands with a few rows of anisorhizas. Unlike calycophorans, they lack paired elongate microbasic mastigophores. Instead, they bear 3 elongated stenoteles, and their cnidobands are followed by a branched vesicle, unique to this genus. Their tentillum morphology is very different from that of other related physonects, which tend to have long, coiled, cnidobands with many paired oval stenoteles. Most calycophoran diet studies have reported their prey to be small crustaceans such as copepods or ostracods. The diet of *Frillagalma vityazi* is unknown, but this morphological convergence presents the hypothesis that they evolved to capture similar kinds of prey. Our DAPCs predict that *Frillagalma* has a generalist niche with both soft and hard bodied prey, including copepods.

Evolution of nematocyst shape – The phylogenetic placement of siphonophores among the Hydrozoa remains an unresolved question (Munro et al. 2018). The most recent work on this front sets them as sister group to all other Hydroidolina (Kayal et al. 2015). All reconstructions of hydrozoan relationships recover siphonophores as an early diverging lineage within Hydroidolina, with many unique apomorphic characters. Therefore, there is a great uncertainty around the ancestral plesiomorphies of the common ancestor of all siphonophores. This is especially true for those characters that present extreme differences between Cystonectae and Codonophora (the earliest split in the siphonophore phylogeny). One of such characters is the shape of haploneme nematocysts. A remarkable feature of siphonophore haplonemes is that they are outliers to all other Medusozoa in their surface area to volume relationships, deviating significantly from sphericity (Thomason 1988). This suggests a different mechanism for their discharge that could be more reliant on capsule tension than on osmotic potentials (Carré and Carré 1980), and strong selection for efficient nematocyst packing in the cnidoband (Thomason 1988; Skaer 1988). Our results show that Codonophora underwent a shift towards elongation and Cystonectae towards sphericity, assuming the common ancestor had an intermediate state. Since we know that the haplonemes of other hydrozoan outgroups are generally spheroid, it is more parsimonious to assume that cystonects are retaining this ancestral state. Later, we observe a return to more rounded (ancestral) haplonemes in *Erenna*, associated with a secondary gain of a piscivorous trophic niche, like that exhibited by cystonects.

Simultaneous with this shift in haploneme shape, heteroneme shape evolution also presents a single transition to elongation. In addition, the clade defined by the most recent common ancestor of *Agalma* and *Nanomia* shows an increased rate of divergence for heteroneme shape, spanning extremes (from oval *Nanomia*

stenoteles to the elongate *Agalma okenii* stenoteles) in relatively short evolutionary time. While cystonects don't bear heteronemes in their tentacles, *Physalia physalis* bears stenoteles in other zooids, hypothetically used for defense rather than for prey capture. These stenotele heteronemes are rounded like those found in pyrostephids and apolemiids, which is consistent with the story of a single transition leading to the elongated heteronemes in the stem of Tendiculophora.

The implications of these results to the evolution of nematocyst function suggests that an innovation in the discharge mechanism of haplonemes may have occurred during the main shift to elongation. Elongate nematocysts can be tightly packed into cnidobands. We hypothesize this may be a Tendiculophora lineage-specific adaptation to packing more nematocysts into a limited tentillum space, as suggested by (Skaer 1988). Tendiculophora is the most abundant, speciose and diverse (ecologically and morphologically) clade of siphonophores, containing Euphysonectae and Calycophorae. We hypothesize that this packing-efficient haploeme morphology may have been a key innovation leading to the diversification of this clade. However, other characters that shifted concurrently in the stem of this clade may have been responsible for their extant diversity.

Diversity of discharge dynamics – A fundamental corollary in functional morphology is that structural morphology determines functional performance (Wainwright and Reilly 1994). We expected the discharge dynamics exhibited by siphonophore tentilla should vary accordingly with their morphological diversity. Our results are consistent with this expectation, where we observe, for example, that cnidoband size largely determines cnidoband discharge speed. This suggests that prey escape response speed may determine the minimum cnidoband length for successful capture.

Insights from tentilla morphology – The measurements taken illustrate that the morphological diversity of siphonophore tentilla and nematocysts pervades across clades, from the overall shape and size, to the dimensions of the nematocysts. Siphonophores bear the largest nematocysts among Hydrozoans, and present a wide variety of nematocyst sizes within the clade. The largest nematocysts in our dataset (*Bargmannia lata* by volume and *Resomia dunnii* by length), are the largest of all nematocysts reported for cnidarians, and therefore possibly the largest intracellular organelles among all living things.

In addition to the insights produced in this study, the newly collected morphological data provide a unique resource for future studies, and a reference dataset for siphonophore identification. Many conspicuous categorical characters in siphonophore tentilla are very diagnostic, such as: the fluorescent lures of *Resomia ornicephala*, the red lures of *Erenna sirena*, the unique cnidoband shapes in different *Erenna* species, the unique branched vesicle of *Frillagalma vityazi*, the medusa-resembling vesicle of *Lychnagalma* with 8 pseudo-tentacles, the zig-zag morphology of *Resomia* species, the inverted orientation of *Physophora* cnidobands, the button-like tentilla of *Physalia*, or the acorn-shaped minute tentilla of *Cordagalma* species (Fig. 9). Some categorical characters are synapomorphic diagnostic characters for large clades, such as the proximal tentillum heteronemes of Eucladophora, the elastic strand, rhopalonemes, and desmonemes of Tendiculophora, the larval tentilla of Euphysonectae, the 2-sized isorhizas of Cystonectae, the saccus canal of Pyrostephidae, or the 7 rows of anisorhizas in Calycophorae. These characters should be used together with the classical nectophore and bract characters to identify species or at least impute phylogenetic affiliation from incomplete material.

Some siphonophore clades have more nematocyst types than others in the tentacles (Tendiculophora has 4 types, Cystonectae and Apolemiidae have 1), or different subtypes (e.g. stenoteles, mastigophores, birhopaloids). Siphonophores bear nematocysts in different parts of the colony (tentacles, gastrozooids, papons, palpacles, bracts, nectophores, and gonozooids) (Totton and Bargmann 1965). In this paper we only look at the presence of nematocyst types in the tentacles, therefore the gains and losses reported are not necessarily morphological innovations, but developmental allocations. For instance, stenoteles (a type of heteroneme) are absent from the tentacles of *Physalia* and seem to reappear in Euphysonectae, but we know that *Physalia* has stenoteles in other body parts (Totton and Bargmann 1965).

Conclusions

Siphonophores play a wide variety of predatory roles in the open ocean, ranging from mid-trophic small crustacean eaters to piscivorous super-carnivores. The morphological attributes of predators are often finely tuned for their performance during the capture of their prey. With the diversification of prey type specializations, comes the evolution of morphologies adapted to the challenges posed by different prey.

Siphonophore tentilla and nematocysts display a plethora of forms, which are strongly associated with their prey type. The results presented here indicate that these associations are a product of correlated evolution in highly integrated traits. We conclude that the siphonophores were able to establish as abundant oceanic predators by occupying a variety of trophic niches through the evolution and diversification of extraordinary prey capture tools on their tentacles.

Supplementary Materials

Data available from the Dryad Digital Repository: <http://dx.doi.org/10.5061/dryad.NNNN>

Funding

This work was supported by the Society of Systematic Biologists (Graduate Student Award to A.D.S.); the Yale Institute of Biospheric Studies (Doctoral Pilot Grant to A.D.S.); and the National Science Foundation (Waterman Award to C.W.D., and NSF-OCE 1829835 to C.W.D., S.H.D.H., and Anela Choy). A.D.S. was supported by a Fulbright Spain Graduate Studies Scholarship.

Acknowledgements

We wish to thank the crew and scientists onboard the R/V Western Flyer, who participated in the collection of many of the specimens used in this study. We also want to thank Lynne Christianson and Shannon Johnson from the Monterey Bay Aquarium Research Institute for their assistance in the field as well as for sequencing some of the species included in this phylogeny. In addition, we wish to thank Lourdes Rojas, Daniel Drew, and Eric Lazo-Wasem for their assistance in imaging the fixed specimens and managing the collections. We thank Dennis Pilarczyk for organizing the prey selectivity data, and Joaquin Nunez for reviewing this manuscript. Finally, we thank Philip Pugh, who confirmed many of our specimen identifications and taught us invaluable knowledge about siphonophores.

Author contributions

Alejandro Damian-Serrano (Yale University) collected specimens and morphological data, executed phylogenetic analyses (tree inference and character evolution), elaborated the figures, wrote and reviewed the manuscript.

Steven H.D. Haddock (Monterey Bay Aquarium Research Institute) contributed by facilitating the access to the field and collection tools, directing the ROV and blue water diving operations in the field. He also contributed extensive knowledge of the biology and ecology of the organisms, and reviewed the manuscript. The Haddock Lab contributed by sequencing many of the species included in the phylogeny presented here.

Elizabeth D. Hetherington and C. Anela Choy (Scripps Institute of Oceanography) contributed by collating the literature and deep-sea video annotation data on siphonophore feeding observations, and by reviewing the manuscript.

Casey W. Dunn (Yale University) contributed by collecting specimens, providing me with invaluable insights and mentoring, and by reviewing the manuscript. In addition, his graduate dissertation work produced many of the sequences used for our phylogenetic analysis.

References

- Adams D.C., Collyer M., Kaliontzopoulou A., Sherratt E. 2016. Geomorph: Software for geometric morphometric analyses.
- Andersen O.G.N. 1981. Redescription of *marrus orthocanna* (kramp, 1942)(Cnidaria, siphonophora). Zoological Museum, University of Copenhagen.
- Bardi J., Marques A.C. 2007. Taxonomic redescription of the portuguese man-of-war, *physalia physalis* (cnidaria, hydrozoa, siphonophorae, cystonectae) from brazil. Iheringia. Série Zoologia. 97:425–433.
- Beaulieu J., O'Meara B. 2012. OUwie: Analysis of evolutionary rates in an ou framework. r package version 1.17.
- Biggs D.C. 1977. Field studies of fishing, feeding, and digestion in siphonophores. Marine & Freshwater

- Behaviour & Phy. 4:261–274.
- Blomberg S.P., Garland T., Ives A.R. 2003. Testing for phylogenetic signal in comparative data: Behavioral traits are more labile. *Evolution*. 57:717–745.
- Blyth C.R. 1972. On simpson's paradox and the sure-thing principle. *Journal of the American Statistical Association*. 67:364–366.
- Butler M.A., King A.A. 2004. Phylogenetic comparative analysis: A modeling approach for adaptive evolution. *The American Naturalist*. 164:683–695.
- Carré D. 1972. Study on development of cnidocysts in gastrozooids of muggiaeae kochi (will, 1844) (siphonophora, calycophora). *Comptes Rendus Hebdomadaires des Seances de l'Academie des Sciences Serie D*. 275:1263.
- Carré D., Carré C. 1980. On triggering and control of cnidocyst discharge. *Marine & Freshwater Behaviour & Phy*. 7:109–117.
- Choy C.A., Haddock S.H., Robison B.H. 2017. Deep pelagic food web structure as revealed by in situ feeding observations. *Proceedings of the Royal Society B: Biological Sciences*. 284:20172116.
- Collins T.J. 2007. ImageJ for microscopy. *Biotechniques*. 43:S25–S30.
- Costello J.H., Colin S.P., Gemmell B.J., Dabiri J.O., Sutherland K.R. 2015. Multi-jet propulsion organized by clonal development in a colonial siphonophore. *Nature communications*. 6:8158.
- David C.N., Özbek S., Adamczyk P., Meier S., Pauly B., Chapman J., Hwang J.S., Gojobori T., Holstein T.W. 2008. Evolution of complex structures: Minicollagens shape the cnidarian nematocyst. *Trends in genetics*. 24:431–438.
- Dunn C.W., Pugh P.R., Haddock S.H. 2005. Molecular phylogenetics of the siphonophora (cnidaria), with implications for the evolution of functional specialization. *Systematic biology*. 54:916–935.
- Felsenstein J. 1985. Phylogenies and the comparative method. *The American Naturalist*. 125:1–15.
- Futuyma D.J., Moreno G. 1988. The evolution of ecological specialization. *Annual review of Ecology and Systematics*. 19:207–233.
- Grafen A. 1989. The phylogenetic regression. *Philosophical Transactions of the Royal Society of London. B, Biological Sciences*. 326:119–157.
- Haddock S.H., Dunn C.W., Pugh P.R., Schnitzler C.E. 2005. Bioluminescent and red-fluorescent lures in a deep-sea siphonophore. *Science*. 309:263–263.
- Haddock S.H., Heine J.N. 2005. Scientific blue-water diving. California Sea Grant College Program.
- Hansen T.F., Martins E.P. 1996. Translating between microevolutionary process and macroevolutionary patterns: The correlation structure of interspecific data. *Evolution*. 50:1404–1417.
- Hardin G. 1960. The competitive exclusion principle. *science*. 131:1292–1297.
- Harmon L.J., Losos J.B., Jonathan Davies T., Gillespie R.G., Gittleman J.L., Bryan Jennings W., Kozak K.H., McPeek M.A., Moreno-Roark F., Near T.J., others. 2010. Early bursts of body size and shape evolution are rare in comparative data. *Evolution: International Journal of Organic Evolution*. 64:2385–2396.
- Harmon L.J., Weir J.T., Brock C.D., Glor R.E., Challenger W. 2007. GEIGER: Investigating evolutionary radiations. *Bioinformatics*. 24:129–131.
- Hessinger D.A. 1988. Nematocyst venoms and toxins. *The biology of nematocysts*. Elsevier. p. 333–368.
- Hissmann K. 2005. In situ observations on benthic siphonophores (physonectae: Rhodaliidae) and descriptions of three new species from indonesia and south africa. *Systematics and Biodiversity*. 2:223–249.
- Höhma S., Landis M.J., Heath T.A., Boussau B., Lartillot N., Moore B.R., Huelsenbeck J.P., Ronquist F. 2016. RevBayes: Bayesian phylogenetic inference using graphical models and an interactive model-specification language. *Systematic Biology*. 65:726–736.
- Hutchinson G.E. 1961. The paradox of the plankton. *The American Naturalist*. 95:137–145.
- Jacobs J. 1974. Quantitative measurement of food selection. *Oecologia*. 14:413–417.
- Jombart T., Devillard S., Balloux F. 2010. Discriminant analysis of principal components: A new method for the analysis of genetically structured populations. *BMC genetics*. 11:94.
- Kalyaanamoorthy S., Minh B.Q., Wong T.K., Haeseler A. von, Jermiin L.S. 2017. ModelFinder: Fast model selection for accurate phylogenetic estimates. *Nature methods*. 14:587.
- Katoh K., Misawa K., Kuma K.-i., Miyata T. 2002. MAFFT: A novel method for rapid multiple sequence alignment based on fast fourier transform. *Nucleic acids research*. 30:3059–3066.
- Kayal E., Bentlage B., Cartwright P., Yanagihara A.A., Lindsay D.J., Hopcroft R.R., Collins A.G. 2015. Phylogenetic analysis of higher-level relationships within hydroidolina (cnidaria: Hydrozoa) using

- mitochondrial genome data and insight into their mitochondrial transcription. *PeerJ*. 3:e1403.
- Lande R. 1976. Natural selection and random genetic drift in phenotypic evolution. *Evolution*. 30:314–334.
- Longhurst A.R. 1985. The structure and evolution of plankton communities. *Progress in Oceanography*. 15:1–35.
- Mackie G.O., Pugh P.R., Purcell J.E. 1987. Siphonophore Biology. *Advances in Marine Biology*. 24:97–262.
- Mapstone G.M. 2014. Global diversity and review of siphonophorae (cnidaria: Hydrozoa). *PLoS One*. 9:e87737.
- Martins E.P. 1996. Phylogenies, spatial autoregression, and the comparative method: A computer simulation test. *Evolution*. 50:1750–1765.
- Mitra A. 2009. Are closure terms appropriate or necessary descriptors of zooplankton loss in nutrient–phytoplankton–zooplankton type models? *Ecological Modelling*. 220:611–620.
- Munro C., Siebert S., Zapata F., Howison M., Serrano A.D., Church S.H., Goetz F.E., Pugh P.R., Haddock S.H., Dunn C.W. 2018. Improved phylogenetic resolution within siphonophora (cnidaria) with implications for trait evolution. *Molecular Phylogenetics and Evolution*.
- Nguyen L.-T., Schmidt H.A., Haeseler A. von, Minh B.Q. 2014. IQ-tree: A fast and effective stochastic algorithm for estimating maximum-likelihood phylogenies. *Molecular biology and evolution*. 32:268–274.
- O’Brien T.D. 2007. COPEPOD, a global plankton database: A review of the 2007 database contents and new quality control methodology.
- Pagel M. 1994. Detecting correlated evolution on phylogenies: A general method for the comparative analysis of discrete characters. *Proceedings of the Royal Society of London. Series B: Biological Sciences*. 255:37–45.
- Paradis E., Blomberg S., Bolker B., Brown J., Claude J., Cuong H.S., Desper R. 2019. Package “ape”. *Analyses of phylogenetics and evolution*, version.:2–4.
- Pennell M.W., FitzJohn R.G., Cornwell W.K., Harmon L.J. 2015. Model adequacy and the macroevolution of angiosperm functional traits. *The American Naturalist*. 186:E33–E50.
- Pigliucci M. 2003. Phenotypic integration: Studying the ecology and evolution of complex phenotypes. *Ecology Letters*. 6:265–272.
- Pugh P. 2001. A review of the genus erenna bedot, 1904 (siphonophora, physonectae). *BULLETIN-NATURAL HISTORY MUSEUM ZOOLOGY SERIES*. 67:169–182.
- Pugh P., Youngbluth M. 1988. Two new species of prayine siphonophore (calycophorae, prayidae) collected by the submersibles johnson-sea-link i and ii. *Journal of Plankton Research*. 10:637–657.
- Purcell J. 1981. Dietary composition and diel feeding patterns of epipelagic siphonophores. *Marine Biology*. 65:83–90.
- Purcell J., Mills C. 1988. The correlation of nematocyst types to diets in pelagic hydrozoa. in “the biology of nematocysts”.(Eds da hessinger and hm lenhoff.) pp. 463–485.
- Purcell J.E. 1980. Influence of siphonophore behavior upon their natural diets: Evidence for aggressive mimicry. *Science*. 209:1045–1047.
- Purcell J.E. 1984. The functions of nematocysts in prey capture by epipelagic siphonophores (coelenterata, hydrozoa). *The Biological Bulletin*. 166:310–327.
- Rabosky D.L., Grunbler M., Anderson C., Title P., Shi J.J., Brown J.W., Huang H., Larson J.G. 2014. BAMM tools: An r package for the analysis of evolutionary dynamics on phylogenetic trees. *Methods in Ecology and Evolution*. 5:701–707.
- Revell L.J. 2012. Phytools: An r package for phylogenetic comparative biology (and other things). *Methods in Ecology and Evolution*. 3:217–223.
- Revell L.J., Chamberlain S.A. 2014. Rphylip: An r interface for phyliip. *Methods in Ecology and Evolution*. 5:976–981.
- Robison B.H. 2004. Deep pelagic biology. *Journal of experimental marine biology and ecology*. 300:253–272.
- Schindelin J., Arganda-Carreras I., Frise E., Kaynig V., Longair M., Pietzsch T., Preibisch S., Rueden C., Saalfeld S., Schmid B., others. 2012. Fiji: An open-source platform for biological-image analysis. *Nature methods*. 9:676.
- Schlüter D. 2000. Ecological character displacement in adaptive radiation. *the american naturalist*. 156:S4–S16.
- Schmitz O. 2017. Predator and prey functional traits: Understanding the adaptive machinery driving

- predator-prey interactions. F1000Research. 6.
- Shapiro S.S., Wilk M.B. 1965. An analysis of variance test for normality (complete samples). Biometrika. 52:591–611.
- Siebert S., Pugh P.R., Haddock S.H., Dunn C.W. 2013. Re-evaluation of characters in apolemidae (siphonophora), with description of two new species from monterey bay, california. Zootaxa. 3702:201–232.
- Simpson G.G. 1955. Major features of evolution. Columbia University Press: New York.
- Skaer R. 1988. The formation of cnidocyte patterns in siphonophores. Academic Press New York.
- Skaer R. 1991. Remodelling during the development of nematocysts in a siphonophore. Hydrobiologia. 216:685–689.
- Sugiura N. 1978. Further analysts of the data by akaike's information criterion and the finite corrections: Further analysts of the data by akaike's. Communications in Statistics-Theory and Methods. 7:13–26.
- Team R.C. 2017. R: A language and environment for statistical computing. vienna, austria: R foundation for statistical computing; 2017.
- Thomason J. 1988. The allometry of nematocysts. The biology of nematocysts. Elsevier. p. 575–588.
- Totton A.K., Bargmann H.E. 1965. A synopsis of the siphonophora. British Museum (Natural History).
- Uhlenbeck G.E., Ornstein L.S. 1930. On the theory of the brownian motion. Physical review. 36:823.
- Uyeda J.C., Zenil-Ferguson R., Pennell M.W. 2018. Rethinking phylogenetic comparative methods. Systematic Biology. 67:1091–1109.
- Wagner G.P., Schwenk K. 2000. Evolutionarily stable configurations: Functional integration and the evolution of phenotypic stability. Evolutionary biology. Springer. p. 155–217.
- Wainwright P.C., Reilly S.M. 1994. Ecological morphology: Integrative organismal biology. University of Chicago Press.